A new measurement of the cosmic ray antiproton spectrum between 80 MeV and 14 GeV

A. Bruno* **and P. Hofverberg†**
on behalf of the PAMELA collaboration

**University of Bari and INFN Sezione di Bari*
Bari, Italy. Alessandro.Bruno@ba.infn.it
†Max-Planck-Institute für Khernphysik
Heidelberg, Germany. Petter.Hofverberg@mpi-hd.mpg.de

***Abstract*. A new measurement of the cosmic ray antiproton absolute flux between 80 MeV and 14 GeV is presented. Data were collected by the satellite-borne experiment PAMELA, devoted to the study of the cosmic radiation with the focus on antiparticles. The apparatus, launched into orbit on-board the Resurs-DK1 satellite on 15 June 2006, consists of a central permanent magnetic spectrometer, an electromagnetic calorimeter, a time-of-flight system, a neutron detector and an anticoincidence shield. Thanks to its high identification capabilities and to the long duration of the mission, PAMELA is measuring cosmic ray antiprotons with unprecedented both statistical precision and explored energy range, thus placing stricter constraints to the existence of exotic processes and to propagation parameters of cosmological models.**

***Keywords*: Antiprotons, cosmic rays, satellite experiments.**

I. INTRODUCTION

PAMELA (a "Payload for Antimatter Matter Exploration and Light-nuclei Astrophysics" [1]) is a satellite-borne experiment conceived to study charged particles in the cosmic radiation. It is in orbit since June 15^{th} 2006 when the Resurs-DK1 satellite, which hosts the apparatus, has been launched into space from the Baikonur cosmodrome, in Kazakhstan.

PAMELA represents the state-of-the-art apparatus for the investigation of cosmic rays. In particular, it has been designed and optimized to measure antiprotons and positrons in a wide energy range, and with high precision and sensitivity, also favored by the satellite semi-polar (70^o inclination) and elliptical ($350 \div 610$ km altitude) orbit, which allows PAMELA to collect a high number of antiparticles in a very clean environment and to extend its observational energy range from tens of MeV up to some hundreds of GeV.

The PAMELA apparatus consists of a set of specialized detectors which allow to determine particles identity and rigidity. The instrument is about 1.3 m high, with a mass of 470 kg and an average power consumption of 355 W. A schematic view of the PAMELA experimental setup is given in Figure 1.

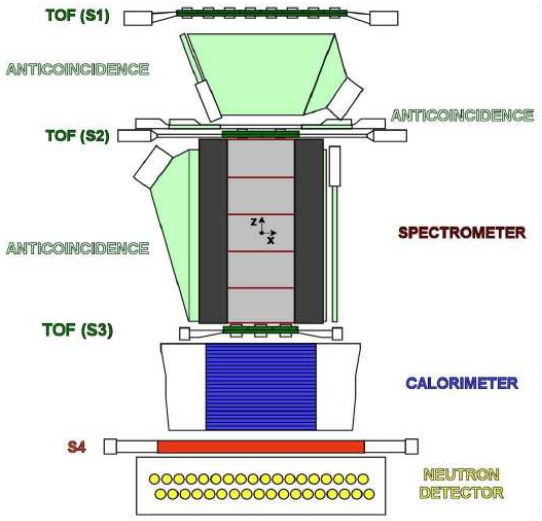

Fig. 1: Schematic drawing of the PAMELA apparatus, showing sensitive areas of the various subdetectors to scale, in a longitudinal section. The right-handed coordinate system used in the experiment is also represented.

The main component is the central magnetic spectrometer, which consists of a hollow 0.43 T permanent magnet and of a set of six high precision double-sided silicon planes. It reconstructs particle curvature by means of impact position on the tracking planes, allowing accurate rigidity and charge measurements.

An electromagnetic calorimeter is located below the spectrometer. It is composed of 22 modules each made up of a central Tungsten absorber sandwiched between two singlesided silicon sensor planes.The total thickness of W absorbers corresponds to 16.3 radiation lengths and to 0.6 interaction lengths. Its high granularity allows a fine reconstruction of the particle shower with high lepton/hadron discrimination capabilities.

A time of flight measurement (ToF) is performed by a set of fast plastic scintillators arranged in three planes, which also provide the rejection of albedo events and allow to determine the absolute value of charge z of incident particles through the multiple measurement of energy loss dE/dx in the scintillator counters. More-

over, the ToF system provides a fast signal for triggering data acquisition in the whole instrument.

An anticounters system (AC), composed of three groups of scintillators (CARD, CAT, CAS), allows rejection of particles whose trajectories are not fully contained in the acceptance window of the spectromenter. A further scintillator planes and a neutron detector (ND) are placed below the calorimeter, in order to provide additional information about shower extension and to improve lepton/hadron discrimination.

II. Event selection

The particle identification with the PAMELA experiment is based on a good track determination provided by the tracking system, fundamental to achieve a reliable estimation of the particle rigidity. A large fraction of events with additional particles in the acceptance is rejected by using a combination of the tracker, the ToF system and anticounters, while a set of cuts are applied on the track reconstruction to assure an accurate charge sign separation and a precise rigidity measurement. The analysis of the interaction topology in the calorimeter is crucial to allow hadron-lepton discrimination. The amount of ionization in the tracker and the ToF planes is used to discard multiply charged particles, and to identify particles with different mass at low rigidity together with the velocity measurement provided by the ToF system.

III. Antiproton identification

High identification capabilities have to be provided for disentangling the rare antiproton signal from the much larger fluxes of cosmic protons and electrons, whose intensities exceed the antiproton flux between $1 \div 10$ GeV by more than respectively four and two orders of magnitude. Consequently, a reliable selection of the rare antiproton component needs strong constrains on the combined information from the several detectors of PAMELA. Opportune selection criteria were developed in order to get a clean antiproton sample from the recorded data. After having been reconstructed, particles were then subject of series of cuts aimed to remove wrongly identified events.

A minimum number of position measurements was required, in order to minimize the uncertainty on the tracking fit and therefore on the rigidity measurement: the used configuration is based on at least four measurements for the bending (X) view and at least three for the non-bending (Y) one. Strict conditions were applied to reject protons which were wrongly reconstructed as negatively charged particles due to scattering. The minimum track quality was improved using a rigidity dependent upper limit on the χ^2 associated to the tracking fit. Indeed, geometrical constraints were imposed to assure the track containment inside the geometrical acceptance of the apparatus.

The calorimeter information was used to reject electrons. The used criteria are based on the longitudinal and transverse segmentation of the calorimeter which, combined with dE/dx measurements from the individual silicon strips, allowed electromagnetic showers to be identified with very high accuracy. An energy dependent set of cuts, developed by means of particle beams and simulations [2], was used to select protons from positrons and, moreover, to identify antiprotons from the dominant electron background, with a resulting contamination estimated to be negligible across the whole energy range of interest. It was developed on basis of the several features describing an electromagnetic shower: i) the starting point of the shower; ii) the longitudinal profile; iii) the transverse profile; iv) the topological development of the shower; v) the energy-momentum match. As example, in Figure 2 is reported the distribution of the $noint$ variable correlated to the starting point of the shower: electromagnetic showers have a high probability to start developing in the first planes of the calorimeter so they are usually characterized by low $noint$ values, while a non-interacting (anti)proton or an (anti)proton interacting after a few planes usually results in higher values of such variable.

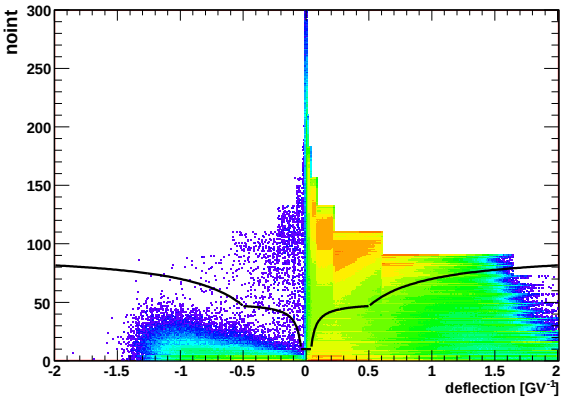

Fig. 2: Distribution of the $noint$ variable, correlated to the shower starting point in the calorimeter. Particles above the black lines are selected as (anti)proton candidates.

A set of further specific selections was developed to assure the correct event reconstruction inside the apparatus, availing of information from the different detectors. The ToF segmentation was used to discard events whose topology did not correspond to single track primary events: a limit on number of hit paddles in the $S1$ and $S2$ scintillator layers was imposed, and only events with not more than one hit paddle per layer and at least one hit paddle per plane, consistent with an extrapolated track from the spectrometer, were selected. Furthermore, multiply charged tracks were rejected by requiring no spurious signals in both the ToF and the tracking system, and no activity in the CARD and CAT anticoincidence scintillators; instead, no constraint was applied to the CAS anticoincidence which, differently from the others, can be activated also by backscattered particles produced in the calorimeter.

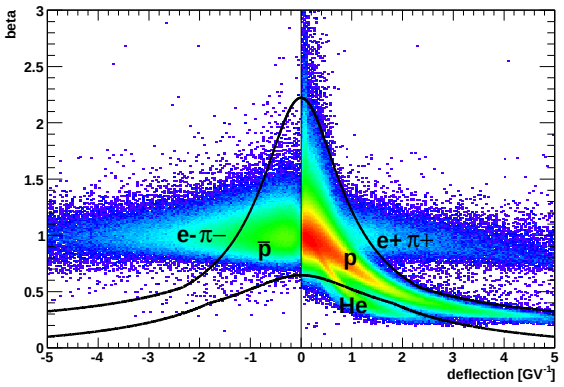

Fig. 3: The velocity (β) versus deflection distribution. Particles within the black lines are selected as (anti)proton candidates.

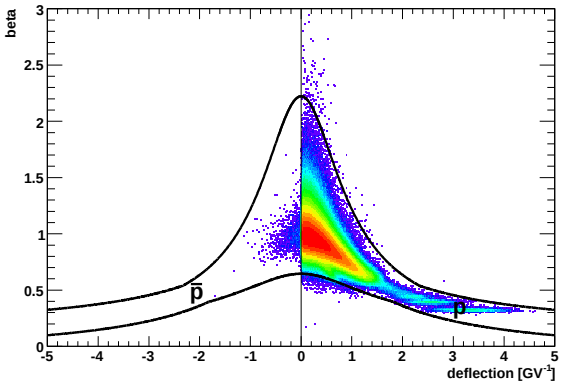

Fig. 4: The velocity (β) versus deflection distribution, obtained after having applied the tracker selection, the charge selection performed with the ToF and the tracker, and the calorimeter selection. Particles within the black lines are selected as (anti)proton candidates.

The particle velocity measurement provided by the ToF and the ionization loss in the tracker silicon planes and in the ToF scintillators were used to reject electrons, pions and wrongly reconstructed events (see Figures 3 and 4). An additional condition was applied to discard events with a still relatively high $S1$ energy deposit, which is typically related to an inelastic reaction occurred in the upper parts of the apparatus, in particular with the PAMELA pressurized container ($\sim$ 2 mm aluminium window).

Particles of not galactic origin (secondary and radiation belt trapped particles) were discarded by selecting only events whose reconstructed rigidity exceeded the vertical geomagnetic cut-off, estimated using the satellite position, by a factor of 1.2 and of 1.3 respectively below and above 3 GeV. Downward-going particles were selected using the ToF information: the time-of-flight resolution of 300 ps ensures that no contamination from albedo particles remains in the selected sample.

IV. Selection efficiencies

Selection efficiencies were determined using flight data, which naturally include detectors performances, while test beam and simulation data were used to support the calculation by cross-checking results. Due to the practical limit of selecting an unbiased, statistically significant antiproton sample to be used, efficiencies were calculated from a flight proton sample once assumed an identical response of the apparatus for protons and antiprotons. Accordingly, each efficiency was derived by selecting an opportune proton sample using all detectors but the one under study.

Methods used to estimate efficiencies depend on the rigidity range [3], [4]. The efficiency of the tracker selection were derived by selecting a proton sample with the ToF, the AC and the calorimeter. Particle tracks were reconstructed in the calorimeter and then back-propagated through the PAMELA acceptance and required to be inside the cavity fiducial volume. Trajectories were approximated as straight lines, with a relative uncertainty estimated with simulation to be negligible in the rigidity region of interest. A specific limit on number of hit paddles in the ToF scintillator layers was applied to discard events whose topology does not correspond to single track primary events, while dE/dx measurements with the ToF system and the first calorimeter plane, respectively below and above 3 GeV, were used to separate protons from multiple charged particles. Below $\sim$ 1 GeV the particles rigidity was reconstructed measuring the velocity with the ToF and assuming a proton mass. Above such threshold the tracker efficiency was found to show no significant variation with rigidity.

The ToF efficiency was obtained by applying the ToF selection criteria on the efficiency sample derived selecting in-acceptance single track events using the tracking system, the AC and the calorimeter, and requiring no spurious signals in the tracker planes and strict constraints on the track quality. Analogously, the other selection efficiencies were calculated by applying the specific selection on a data sample derived independently using all the other detectors. The approximation of calculating efficiencies using a proton sample is considered satisfying for all detectors except for the calorimeter, due to differences related to hadronic cross sections between $\bar{p}$ and p, which were properly taken into account by means of a correction factor calculated with simulations.

V. The $\bar{p}$ flux

The number of antiprotons at the top of atmosphere was obtained by compensating the number of selected antiproton candidates by the following effects: i) pion contamination, ii) the selection efficiencies, iii) the energy loss and the percentage of the particle lost by hadronic interactions in the instrument, iv) the geometrical factor of the apparatus and v) the particle transmission through the geomagnetic field.

The contamination from $\pi-$ produced by cosmic ray interactions with the PAMELA payload was studied

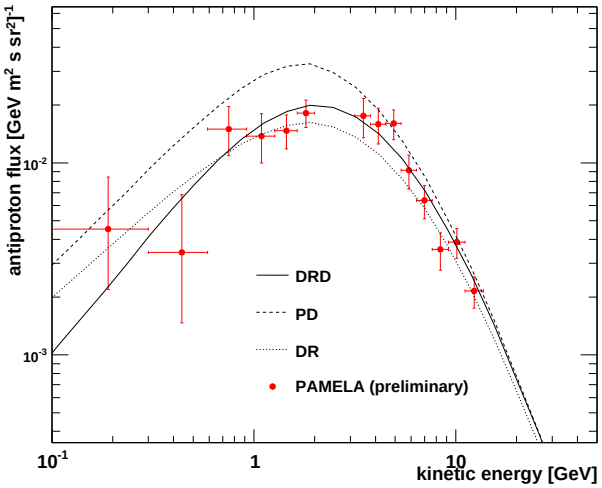

Fig. 5: The antiproton flux measured with the PAMELA instrument. Predictions from some theoretical models describing pure secondary $\bar{p}$ production [8] are also shown for comparison: i) a plain diffusion model with an ad-hoc break in the diffusion coefficient (PD); ii) a distributed re-acceleration and power-law diffusion with no breaks (DR); iii) a new self-consistent model of diffusive re-acceleration with damping (DRD).

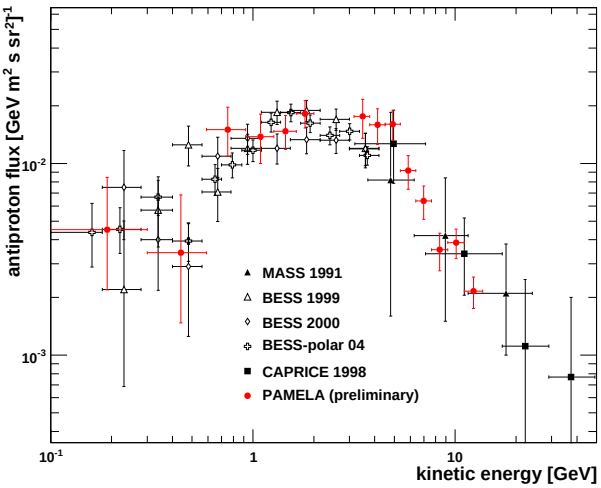

Fig. 6: The antiproton flux measured by PAMELA compared with some recent experimental data: BESS 1999, 2000 and 2004 flights campaigns [9], MASS 1991 [10] and CAPRICE 1998 [11].

using both flight data and accurate simulations [3], [4] based on both GEANT3.21 [5] and FLUKA [6] packages. As a result, a residual pion contamination of less than 5% above 2 GV was estimated, decreasing to less than 1% above 5 GV. Details about methods developed for the background evaluation will be described in a separate paper in this conference [7].

Dedicated simulations were used to estimate the apparatus geometrical factor and the corrections related to the energy loss inside the instrument and the fraction of particles lost due to inelastic reactions.

Finally, the spectrum was corrected for the transmission in the geomagnetic field, which deflects charged particles and can prevent low energy particles from reaching PAMELA. The final flux normalization was obtained by weighting each flux bin by the live time spent by PAMELA at each geomagnetic cut-off lower than the corresponding rigidity value in that bin.

VI. Results

At the time of writing a limited sample of data acquired with a specific trigger configuration and excluding orbital regions characterized by low geomagnetic field values was analyzed, for a total live time of $\sim$ 160 days. A total number of 170 and 211 antiprotons were identified respectively below and above 3 GeV. Data were recorded by PAMELA in the period July 2006 to February 2008. This is a period of minimum solar activity and negative solar polarity and the PAMELA measurement is the first observation of antiprotons during this particular solar state.

The preliminary PAMELA antiproton measurements are presented in Figure 5. Some recent theoretical models describing pure secondary production of antiprotons, but which differ in galactic propagation, are considered for a comparison [8]: i) a plain diffusion model with an ad-hoc break in the diffusion coefficient (PD model); ii) a distributed re-acceleration and power-law diffusion with no breaks (DR model); iii) a new self-consistent model of diffusive re-acceleration with damping (DRD model). PAMELA data are also compared with other recent antiproton measurements in Figure 6: BESS 1999, 2000 and 2004 flights campaigns [9], MASS 1991 [10] and CAPRICE 1998 [11]. Error bars shown in figure include both statistical and the systematic uncertainties. Statistics will be significantly improved with the analysis of the full data sample and of new data acquired by PAMELA up to January 2009, for a total acquisition time of $\sim$ 750 days.

References

[1] P. Picozza et al, Astroparticle Physics, 27, 296, 2007.
[2] M. Boezio *et al.*, Astropart. Phys. 26, 111 (2006).
[3] A. Bruno, Ph.D. thesis, University of Bari, 2008.
[4] P. Hofverberg, Ph.D. thesis, Royal Institute of Technology, Stockholm, 2008.
[5] The GEANT team, "GEANT - Dectector Description and Simulation Tool", The CERN computing center. CERN Program Library Long Writeup W5013.
[6] A. Fassò, A. Ferrari, J. Ranft and P. R. Sala, "FLUKA: Status and Prospective for Hadronic Applications", in Proocedings of the MonteCarlo 2000 Conference, Springer-Verlag, Berlin, 2001, pp. 955-960.
[7] A. Bruno et al., "Estimate of the pion contamination in the PAMELA antiproton measurements", this conference, OG.1.1 384, 2009.
[8] V. S. Ptuskin, I. V. Moskalenko, F. C. Jones *et al.*, "Dissipation of magnetohydrodynamic waves on energetic particles: impact on interstellar turbulence and cosmic ray transport", The Astrophysical Journal 642 902 (2006).
[9] A. Yamamoto, *et al.*, Nucl. Phys. B Proc. Suppl. 166, 62 (2007).
[10] M. Hof *et al.*, Astroph. Jour. 467, L33 (1996). C. Grimani *et al.*, Astr. and Astroph. 392, 287 (2002).
[11] M. Boezio *et al.*, Astroph. Jour. 561, 787 (2001).